



Short communication

Ruthenium based electrocatalysts for hydrogen oxidation, prepared by a microwave assisted method

E. Borja-Arco^{a,*}, O. Jiménez-Sandoval^b, L. Magallón-Cacho^c, P.J. Sebastian^c^a Departamento de Física y Química Teórica, Facultad de Química, Universidad Nacional Autónoma de México, Av. Universidad 3000, Ciudad Universitaria, México, D. F. 04510, Mexico^b Centro de Investigación y de Estudios Avanzados del Instituto Politécnico Nacional (Cinvestav), Unidad Querétaro, Apartado Postal 1-798, Querétaro, Qro. 76001, Mexico^c Instituto de Energías Renovables, Universidad Nacional Autónoma de México, Privada Xochicalco S/N, Temixco, Mor. 62580, Mexico

H I G H L I G H T S

- Ruthenium catalysts synthesized by a microwave-assisted method.
- Ruthenium materials as HOR catalysts.
- Potential use of these materials as PEMFC anodes.

A R T I C L E I N F O

Article history:

Received 14 February 2013

Received in revised form

20 July 2013

Accepted 24 July 2013

Available online 2 August 2013

Keywords:

Microwave irradiation

Ruthenium catalysts

Hydrogen oxidation

Polymer electrolyte fuel cell

A B S T R A C T

Ruthenium monometallic electrocatalysts for the hydrogen oxidation reaction (HOR) were prepared by microwave irradiation in *o*-dichlorobenzene and ethylene glycol. The products were characterized structurally by X-ray diffraction and FT-IR spectroscopy; morphologically by scanning electron microscopy and their chemical composition was determined by energy-dispersive spectroscopy analysis. The electrocatalytic properties of the materials were evaluated by rotating disk electrode measurements in 0.5 mol L⁻¹ H₂SO₄. The kinetic parameters, such as the Tafel slope, exchange current density and charge transfer coefficient, are reported. The ruthenium electrocatalysts show a *dual-path* mechanism in a similar way as platinum.

© 2013 Elsevier B.V. All rights reserved.

1. Introduction

The slow kinetics of the oxygen reduction reaction ($j_o \sim 10^{-10}$ – 10^{-12} A cm⁻²) and methanol poisoning at the cathode in a PEMFC and DMFC [1,2], respectively, as well as the CO poisoning at the anode in a PEMFC [3] (showed by platinum electrocatalysts), have resulted in the development of alternative materials to platinum with high activity for the ORR and HOR, but with resistance to the contaminants mentioned above.

Ru-based catalysts are considered a promising alternative to Pt as cathode catalysts in DMFCs (and PEMFCs), due to their tolerance to methanol oxidation. This is attributed to the lack of available surface sites for methanol adsorption due to the strongly adsorbed

oxygenated species [4]. On the other hand, most of the materials reported in the literature for the hydrogen oxidation reaction (HOR) have been based on platinum and their alloys (Pt–Ru, Pt–Mo) [5], Pd alloys (Pd–Au) [6] and more recently, osmium [7]; however, to the best of our knowledge, no ruthenium monometallic catalysts have been studied. Many of such catalysts reported in the literature have been synthesized using a conventional heating method, i.e., organic solvents at their refluxing temperature or by pyrolysis of some metal precursors [8–14]. However, this is a relatively slow and inefficient method for transferring energy into the system because heat passes first through the walls of the vessel in order to reach the solvent and reactants; furthermore, this results in the temperature of the vessel being higher than that of the reaction mixture. On the other hand, microwave energy couples directly with the molecules that are present in the reaction mixture, leading to a rapid rise in temperature; the process is not dependent upon the thermal conductivity of the vessel materials.

* Corresponding author. Tel.: +52 55 56223899.

E-mail addresses: eborja@unam.mx, eborjarco@gmail.com (E. Borja-Arco).

Microwave energy has been employed in many recent chemical reaction studies and has been found to change the kinetics and selectivity, often in favorable ways. These reactions include organic and inorganic syntheses, selective sorption, oxidation/reduction, polymerization, among many other processes [15]. Recently, we have reported [16,17] the use of microwave energy for the synthesis of ruthenium and osmium catalysts for the oxygen reduction reaction (ORR) with an electrochemical behavior similar to that exhibited by materials obtained by a conventional synthesis method. The present article reports on the electrocatalytic activity of Ru materials prepared by a microwave-assisted method for the hydrogen oxidation reaction in an acid medium.

2. Experimental

2.1. Synthesis of the catalysts

The ruthenium electrocatalysts were synthesized using 0.063 mmol of triruthenium dodecacarbonyl [$\text{Ru}_3(\text{CO})_{12}$, Aldrich], mixed with 5 mL of one of two organic solvents: *o*-dichlorobenzene (b.p. 178–180 °C, Aldrich) and ethylene glycol (b.p. 195–198 °C, Aldrich). The mixture was thermally treated using microwave irradiation on an Anton Paar-Monowave reactor 300; experimental conditions are shown in Table 1. The products obtained were washed with 2-propanol (J.T. Baker) and dried at room temperature. The solvents were selected according to their different ability to absorb microwave energy [15].

2.2. Structural characterization of the catalysts

The electrocatalysts synthesized were structurally characterized using reflectance FT-IR spectroscopy on a Perkin–Elmer-GX3 spectrometer, with the samples dissolved in FT-IR grade KBr (Aldrich). For the XRD studies, a Rigaku D/max-2100 diffractometer, with Cu $K\alpha_1$ irradiation (1.5406 Å) was used. A Philips XL30ESEM microscope was used to obtain scanning electron micrographs and X-ray energy-dispersive spectra (EDS) of the catalysts, for surface morphology and chemical composition studies, respectively.

2.3. Electrochemical experiments

2.3.1. Electrode preparation

The electrode for the rotating disk electrode (RDE) studies was prepared by mixing 1.7 mg of Vulcan[®] XC-72 (Cabot) and 0.3 mg of the catalyst with 10 μL of a 5% Nafion[®] solution (ElectroChem) in an ultrasonic bath; 2 μL of the resulting slurry were deposited on the glassy carbon electrode and dried at room temperature. The cross-sectional area of the disk electrode on which the catalyst-support mixture was deposited (geometrical area) was 0.072 cm².

Table 1
Experimental conditions during the microwave assisted synthesis of $\text{Ru}_y\text{-ETG}$ and $\text{Ru}_y\text{-DCB}$.

Step	Program	Temperature °C	Time minutes:seconds	Stirrer
1	Heat to temperature	180	3:00	On
2	Hold	180	30:00	On
3	Heat to temperature	200	5	On
4	Hold	200	1	On
5	Heat to temperature	250	5	On
6	Hold	250	4	On
7	Cool down	30	—	On

2.3.2. Equipment

The RDE studies were carried out at room temperature, in a conventional electrochemical cell, with a mercury sulfate electrode ($\text{Hg}/\text{Hg}_2\text{SO}_4/0.5 \text{ mol L}^{-1} \text{ H}_2\text{SO}_4$; abbreviated as MSE) as reference ($\text{MSE} = 0.680 \text{ V/NHE}$), which was connected to the cell through a bridge with a Luggin capillary, and a graphite rod as counter electrode. The potentials were referred to normal hydrogen electrode (NHE). The 0.5 mol L⁻¹ H_2SO_4 solution used as electrolyte was prepared with 98% sulfuric acid (J.T. Baker) and deionized water (18.2 M Ω -cm). A potentiostat/galvanostat (Solartron 1287) and a PC with CorreWare software were used for the electrochemical measurements. A Radiometer Analytical BM-EDI101 glassy carbon rotating disk electrode (with a CTV101 speed control unit) was used for the voltammetry studies.

2.3.3. Electrochemical methods

2.3.3.1. Cyclic voltammetry. Cyclic voltammetry (CV) experiments were done to clean, activate and characterize the electrode surface of ruthenium materials for the HOR. This was done by scanning (in the electrolyte saturated with nitrogen; Infra, UHP) between 0 and 0.98 V/NHE at 20 mV s⁻¹, until no variation in the voltammograms was observed (30 cycles).

2.3.3.2. Hydrogen oxidation reaction (HOR). Linear sweep voltammetry (LSV) was done by saturating the electrolyte with hydrogen (Infra; UHP) for 15 min. Polarization curves were obtained from the open circuit potential in the presence of hydrogen, $E_{\text{oc}}^{\text{H}_2}$, to 0.280 V/NHE. The rotation rates ranged from 100 to 900 rpm.

3. Results

3.1. Structural characterization

Fig. 1 shows the FT-IR spectra of the materials prepared, along with the spectrum of the $\text{Ru}_3(\text{CO})_{12}$ precursor as reference. The latter shows strong carbonyl stretching vibration bands around 2040 cm⁻¹, as well as a group of bands around 570 cm⁻¹, which have been assigned to carbonyl deformation modes, $\delta_{\text{M-CO}}$ [18]. As for the ruthenium catalysts prepared, they do not show any carbonyl bands, inferring that they virtually lose all these groups.

Fig. 2 shows the X-ray diffraction (XRD) patterns of the materials synthesized and the $\text{Ru}_3(\text{CO})_{12}$ precursor as reference.

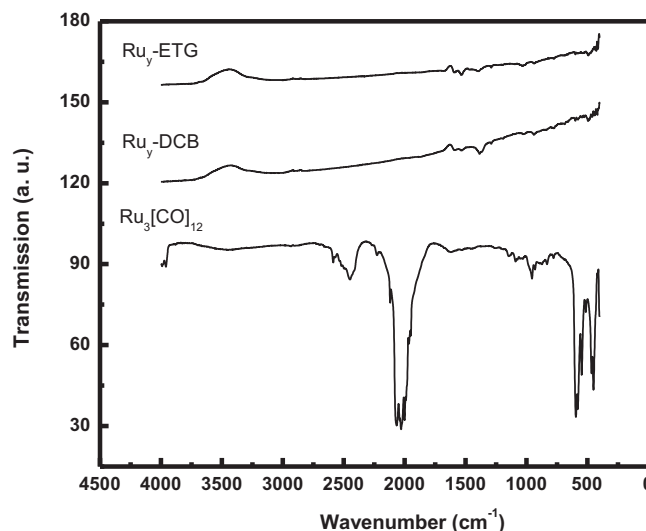


Fig. 1. FT-IR spectra of $\text{Ru}_3(\text{CO})_{12}$ and the ruthenium catalysts synthesized in *o*-dichlorobenzene ($\text{Ru}_y\text{-DCB}$) and ethylene glycol ($\text{Ru}_y\text{-ETG}$).

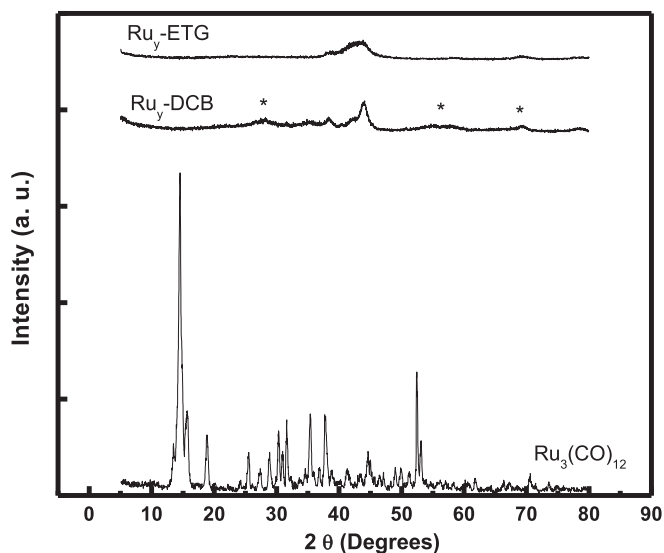


Fig. 2. X-ray diffraction patterns of $\text{Ru}_3(\text{CO})_{12}$ and the ruthenium catalysts synthesized in *o*-dichlorobenzene ($\text{Ru}_y\text{-DCB}$) and ethylene glycol ($\text{Ru}_y\text{-ETG}$). The peaks of RuO_2 have been marked with an asterisk (*).

The catalyst prepared in ethylene glycol ($\text{Ru}_y\text{-ETG}$) shows only metallic ruthenium peaks, $\text{Ru}(0)$, while the material synthesized in *o*-dichlorobenzene ($\text{Ru}_y\text{-DCB}$) also shows low-intensity peaks corresponding to RuO_2 , $\text{Ru}(\text{IV})$. These results are in agreement with their chemical composition determined by EDS (Table 2), which shows that both materials are predominantly formed by ruthenium and small percentages of oxygen and carbon; the higher content of oxygen in $\text{Ru}_y\text{-DCB}$ is consistent with the formation of small amounts of RuO_2 , as observed by XRD; the small content (2.7%) of this element in the other catalyst could be accounted for by the formation of superficial oxygenated Ru species; the presence of residual carbon, presumably from the organic solvents, has been found in previous works where metal based catalysts have been prepared in these media [4]. Table 3 shows the Ru particle size values calculated using the software Jade 6.5; it can be observed that metal nanoparticles were obtained in both solvents, but those synthesized in ethylene glycol are considerably smaller (4 nm), as expected from the corresponding XRD patterns. This is an important property from the viewpoint of electrocatalysis, given the convenience of using large surface areas.

Fig. 3 shows the SEM images of the $\text{Ru}_y\text{-ETG}$ and $\text{Ru}_y\text{-DCB}$ electrocatalysts. The former exhibits a surface morphology composed of round shaped aggregates, while sphere-like particles assembled in larger structures are observed for $\text{Ru}_y\text{-DCB}$.

3.2. Electrochemical characterization

3.2.1. Cyclic voltammetry

The cyclic voltammograms of the ruthenium monometallic electrodes are shown in Fig. 4. It can be observed a cathodic peak in the 0.2–0.4 V/NHE range, which is higher for the catalyst

Table 2

Chemical composition of the ruthenium electrocatalysts determined by EDS studies.

Element	DCB wt %	ETG wt %
C	9.34	4.98
O	5.37	2.70
Ru	85.29	92.32

Table 3

Particle size of the Ru catalysts synthesized in *o*-dichlorobenzene and ethylene glycol.

Solvent	Ru particle size (Å)
DCB	120
ETG	40

synthesized in ethylene glycol than for that synthesized in *o*-dichlorobenzene, where RuO_2 is an important component of the particles. This is in agreement with the observations of Altamirano-Gutiérrez et al. [12], who mention that the electroreduction of thick RuO_2 films, under acidic conditions, is very slow or even impossible to attain, and hence the reduction of RuO_2 is not observed in the cyclic voltammograms of Ru materials containing this oxide.

On the other hand, these materials also show the presence of hydrogen and oxygen evolutions peaks, in the cathodic $\sim 0\text{--}0.1$ V/NHE and anodic $\sim 0.85\text{--}0.95$ V/NHE regions, respectively. This feature is observed for most of the Ru-based catalysts reported in the literature [12–14].

3.2.2. Hydrogen oxidation reaction (LSV)

Fig. 5a shows the polarization curves for hydrogen oxidation of the ruthenium monometallic catalysts synthesized. It can be observed that the current density of the material synthesized in dichlorobenzene is slightly higher than that synthesized in ethylene-glycol. The presence of the metallic oxide in $\text{Ru}_y\text{-DCB}$ could be favoring this reaction as occurs for methanol oxidation [2,3].

In order to obtain the total electroactivity of the materials synthesized from linear sweep voltammetry studies, the kinetic and diffusion currents must be known. According to Koutecky–Levich, the current equation at a given potential is [19]:

$$\frac{1}{i} = \frac{1}{i_k} + \frac{1}{i_l} = \frac{1}{i_k} + \frac{B}{\omega^{1/2}} \quad (1)$$

where i is the measured disk current, i_k the activation or kinetic current, i_l the diffusion control current, ω the angular velocity in revolutions per minute, while

$$B = \frac{1}{0.20nFAD^{2/3}\nu^{-1/6}C} \quad (2)$$

where, n is the number of electrons exchanged per mol of H_2 , F the Faraday constant, A the catalytic effective surface area (cm^2), ν the kinematic viscosity of the electrolyte ($0.01 \text{ cm}^2 \text{ s}^{-1}$), D the hydrogen diffusion coefficient ($3.7 \times 10^{-5} \text{ cm}^2 \text{ s}^{-1}$) and C the bulk hydrogen concentration in the electrolyte ($7.14 \times 10^{-7} \text{ mol cm}^{-3}$). A plot of i^{-1} vs. $\omega^{-1/2}$ at different potentials should yield straight and parallel lines with intercepts corresponding to the inverse of the real kinetic current and slopes yielding the values of B [20].

Normally, the kinetic current values obtained from the interception of Koutecky–Levich plots are used to generate the Tafel curves; however, very precise results may not be obtained due to inevitable variations in the experimental conditions. For this reason, the current–potential curves were corrected in order to get the correct kinetic current. Once obtained an average B at different potentials, it could be obtained the corresponding i_l from different rotation speeds (ω) applied,

$$i_l = \frac{\omega^{1/2}}{B} \quad (3)$$

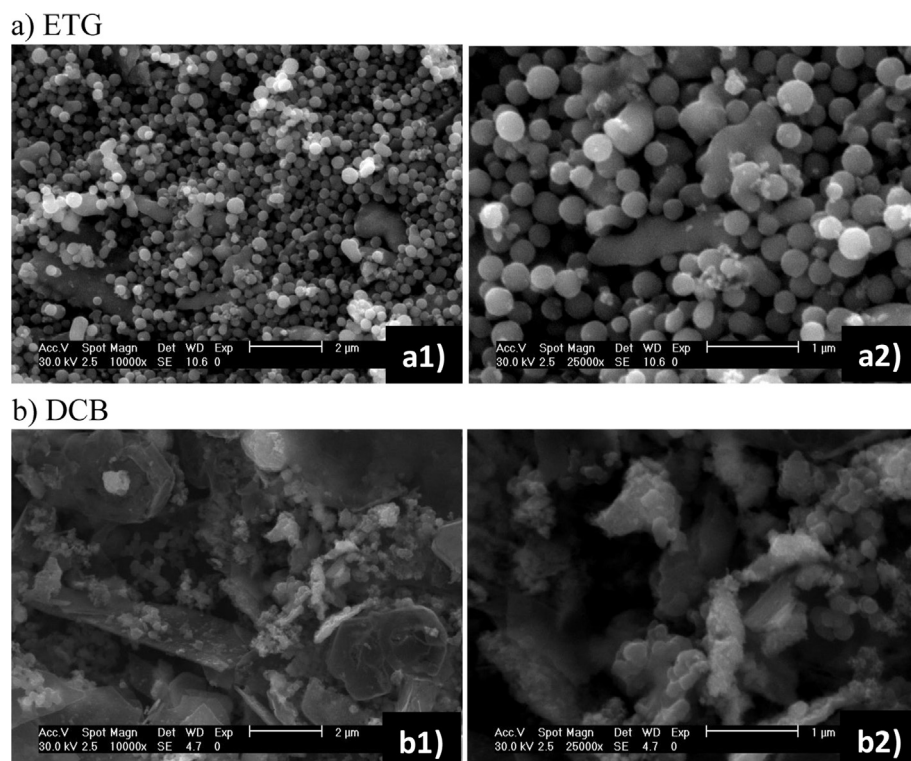


Fig. 3. Scanning electron micrographs of the ruthenium catalysts synthesized in *o*-dichlorobenzene (a1 and a2) and ethylene glycol (b1 and b2), at different magnifications.

and from Eq. (1)

$$i_k = \frac{i_l \cdot i}{i_l - i} \quad (4)$$

i_k was obtained at each ω (100–900 rpm) using Eq. (4). Finally, at each potential applied an average i_k was obtained.

The effective catalytic surface area (A_{eff}) was calculated from Eq. (2), using the average experimental Koutecký–Levich slope, B_{exp} (~ 75 and $\sim 55 \text{ rpm}^{1/2} \text{ mA}^{-1}$ for $\text{Ru}_y\text{-DCB}$ and $\text{Ru}_y\text{-ETG}$, respectively)

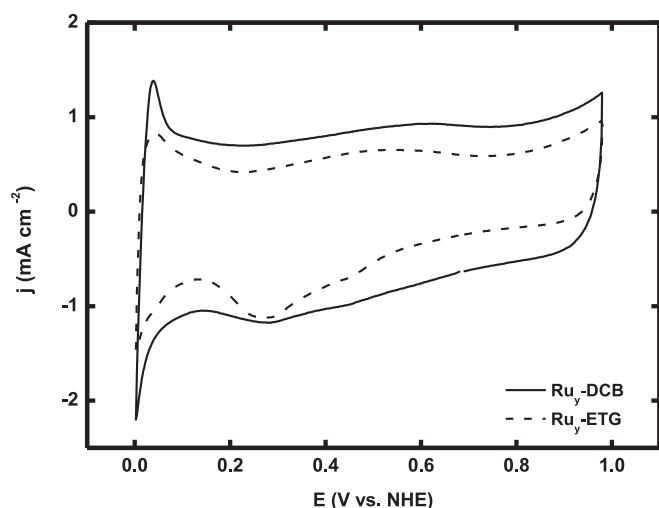


Fig. 4. Cyclic voltammograms of the ruthenium catalysts synthesized in *o*-dichlorobenzene ($\text{Ru}_y\text{-DCB}$) and ethylene glycol ($\text{Ru}_y\text{-ETG}$). The electrolyte was $0.5 \text{ mol L}^{-1} \text{ H}_2\text{SO}_4$ and the sweep rate was 20 mV s^{-1} .

$$A_{\text{eff}} = \frac{1}{0.20nFB_{\text{exp}}v^{-1/6}D_{\text{H}_2}^{2/3}C_{\text{H}_2}} \quad (5)$$

All currents measured, cyclic voltammograms, polarization curves and Tafel plots (exchange current density) were normalized to this effective area.

Table 4 shows the open circuit potential values and HOR kinetic parameters of the ruthenium electrocatalyst and 30% Pt/Vulcan® in H_2 -saturated $0.5 \text{ mol L}^{-1} \text{ H}_2\text{SO}_4$ (obtained experimentally) for comparison, at room temperature. The kinetic parameters were calculated from the corresponding mass corrected Tafel Plots, Fig. 5b. It can be observed that both ruthenium electrodes show an open circuit potential (E_{OC}) equal to that shown by the platinum electrode (0 V/NHE); this fact can be taken as a first sign of the capacity of the novel Ru catalysts to oxidize hydrogen, from a thermodynamic point of view. On the other hand, the experimental Tafel slopes, of ca. $40 \text{ mV decade}^{-1}$ and very similar to the corresponding value for Pt, are in agreement with the theoretical prediction for the Heyrovsky/Volmer mechanism (Eq. (6)), with the Volmer reaction (Eq. (7)) as the rate determining step [21]:



On analyzing the charge transfer coefficient (α) and exchange current density (j_0) values, we can observe that they are of the same order of magnitude for both Ru catalysts, however, j_0 , related with the reaction rate constant, is slightly higher for the $\text{Ru}_y\text{-DCB}$ catalyst, in agreement with the LSV results. Interestingly, both j_0 values are larger than that exhibited by the traditional platinum catalyst and other materials reported in the literature, e.g. Au–Pd alloys [6] and osmium carbonyl catalysts [7]. Another important fact is that

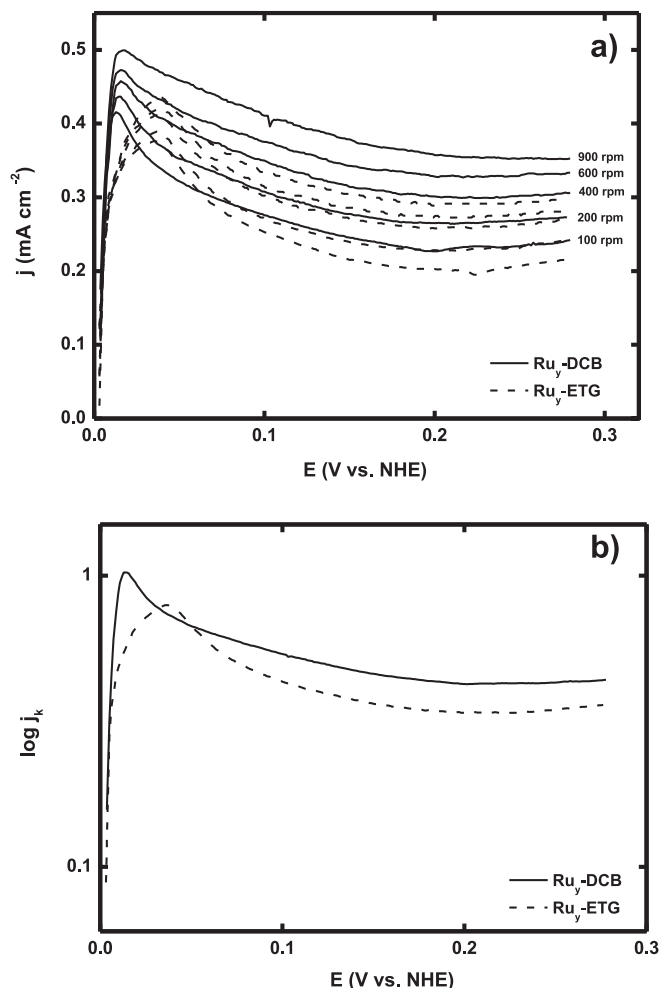


Fig. 5. HOR studies of the ruthenium catalysts synthesized in *o*-dichlorobenzene ($\text{Ru}_\gamma\text{-DCB}$) and ethylene glycol ($\text{Ru}_\gamma\text{-ETG}$): a) Linear sweep voltammetry (sweep rate 5 mV s^{-1}); b) mass corrected Tafel plots. The electrolyte was $0.5 \text{ mol L}^{-1} \text{ H}_2\text{SO}_4$.

Table 4

Open circuit potential values and HOR kinetic parameters of the ruthenium electrocatalysts in H_2 -saturated $0.5 \text{ mol L}^{-1} \text{ H}_2\text{SO}_4$, at room temperature.

Electrocatalyst	E_{oc} V/NHE	b mV decade $^{-1}$	α	j_0 mA cm^{-2}
$\text{Ru}_\gamma\text{-DCB}$	0	39.91	0.5082	0.3211
$\text{Ru}_\gamma\text{-ETG}$	0	40.85	0.4514	0.2907
30% Pt/Vulcan®	0	37.36	0.5837	0.1287

there is very scarce information about the HOR performed by ruthenium catalysts; many of the existing reports focus in different alloys of Pt and Pd [2,5,6].

4. Conclusions

Two ruthenium electrocatalysts for the hydrogen oxidation reaction have been synthesized using a non-conventional method with microwave irradiation assistance. Both catalysts, prepared in different solvents (ethylene glycol and *o*-dichlorobenzene), show similar kinetic parameters, however, $\text{Ru}_\gamma\text{-DCB}$ shows a slightly larger exchange current density, a parameter directly related with the reaction rate constant. The similar or even improved results of these Ru based materials compared with those of traditional Pt/Vulcan® catalysts, render them potential candidates to be evaluated as hydrogen PEM fuel cell anodes with a lower cost. It was confirmed the improvement of the synthesis of these kinds of materials by the use of microwave irradiation, since long preparation times were not necessary, in contrast with conventional methods.

Acknowledgments

This work was supported by CONACYT through project 100212, DGAPA-UNAM through project IN103410 and by PAIP-UNAM through project 3190-22. The authors wish to thank R.A. Mauricio-Sánchez, M.A. Hernández-Landaverde and J.E. Urbina-Alvarez (CINVESTAV-Querétaro), and M. L. Ramón-García (CIE-UNAM) for valuable technical assistance. A Postdoctoral scholarship from CONACYT (L. Magallón-Cacho) is acknowledged as well.

References

- [1] T.R. Ralph, M.P. Hogarth, *Platinum Met. Rev.* 46 (2002) 3–14.
- [2] M.P. Hogarth, T.R. Ralph, *Platinum Met. Rev.* 46 (2002) 146–164.
- [3] T.R. Ralph, M.P. Hogarth, *Platinum Met. Rev.* 46 (2002) 117–135.
- [4] L. Jong-Won, N.P. Branko, *J. Solid State Electrochem.* 11 (2007) 1355–1364.
- [5] A. Pozio, L. Giorgi, E. Antolini, E. Passalacqua, *Electrochim. Acta* 46 (2000) 555–561.
- [6] T.J. Schmidt, V. Stamenkovic, N.M. Markovic, P.M. Ross Jr., *Electrochim. Acta* 48 (2003) 3823–3828.
- [7] J. Uribe-Godínez, R.H. Castellanos, E. Borja-Arco, A. Altamirano-Gutiérrez, O. Jiménez-Sandoval, *J. Power Sources* 177 (2008) 286–295.
- [8] O. Solorza-Feria, S. Durón, *Int. J. Hydrogen Energy* 27 (2002) 451–455.
- [9] V. Trapp, P. Christensen, A. Hamnett, *J. Chem. Soc. Faraday Trans.* 92 (1996) 4311–4319.
- [10] V.L. Rhun, N. Alonso-Vante, *J. New Mater. Electrochem. Syst.* 3 (2000) 333–338.
- [11] E. Borja-Arco, R.H. Castellanos, J. Uribe-Godínez, A. Altamirano-Gutiérrez, O. Jiménez-Sandoval, *J. Power Sources* 188 (2009) 387–396.
- [12] A. Altamirano-Gutiérrez, O. Jiménez-Sandoval, J. Uribe-Godínez, R.H. Castellanos, E. Borja-Arco, J.M. Olivares-Ramírez, *Int. J. Hydrogen Energy* 34 (2009) 7983–7994.
- [13] R.H. Castellanos, E. Borja-Arco, A. Altamirano-Gutiérrez, R. Ortega-Borges, Y. Meas, O. Jiménez-Sandoval, *J. New Mater. Electrochem. Syst.* 8 (2005) 69–75.
- [14] N. Alonso-Vante, H. Tributsch, O. Solorza-Feria, *Electrochim. Acta* 40 (1995) 567–576.
- [15] B.L. Hayes, *Microwave Synthesis, Chemistry at the Speed of Light*, CEM Publishing, 2002.
- [16] E. Borja-Arco, O. Jiménez-Sandoval, J. Escalante-García, A. Sandoval-González, P.J. Sebastian, *Int. J. Hydrogen Energy* 36 (2011) 103–110.
- [17] E. Borja-Arco, O. Jiménez-Sandoval, J. Escalante-García, L. Magallón-Cacho, P.J. Sebastian, *Int. J. Electrochem.* (2011), <http://dx.doi.org/10.4061/2011/830541>. Article ID 830541.
- [18] C.E. Anson, U.A. Jayasooriya, *Spectrochim. Acta* 46A (1990) 861–869.
- [19] Eliezer Gileadi, *Electrode Kinetics for Chemists, Chemical Engineers, and Material Scientists*, VCH Publishers, Inc., New York, 1993.
- [20] Hubert A. Gasteiger, Nenad M. Markovic, Philip N. Ross Jr., *J. Phys. Chem.* 99 (1995) 8290–8301.
- [21] R.M.Q. Mello, E.A. Ticianelli, *Electrochim. Acta* 42 (1997) 1031–1039.